Effects of Resonant Magnetic Perturbations on the dynamics of edge transport barriers

Michael LECONTE[1)], Peter BEYER[1)], Xavier GARBET[2)] and Sadruddin BENKADDA[1)]

[1)] *France-Japan Magnetic Fusion Laboratory LIA 336 CNRS / UMR 6633 CNRS - Université de Provence, France*

[2)] *CEA, IRFM, France*

(Received: 1 September 2008 / Accepted: 7 January 2009)

Recent experimental studies demonstrate a qualitative control over the ELMs by imposing resonant magnetic perturbations at the plasma edge [T.E. Evans, R.A. Moyer, P.R. Thomas et al., Phys. Rev. Lett. 92, 235003 (2004), Y. Liang, H.R. Koslowski, P.R. Thomas et al., Phys. Rev. Lett. 98, 265004 (2007), K. H. Finken, B. Unterberg, Y. Xu et al, Nucl. Fusion 47, 522 (2007)]. However, in order to get any quantitative result, work has to be done in the understanding of ELM dynamics. We present results from numerical simulations of Resistive Ballooning Mode (RBM) reproducing the stabilization of barrier relaxations by a static magnetic perturbation. It is found that this stabilizing effect is linked to the modification of the pressure gradient profile which is due mainly to the presence of a residual magnetic island chain at the position of main resonance.

Keywords: turbulence, transport barriers, resonant magnetic perturbations, stochastic transport

1. Introduction

In divertor tokamak plasmas, an Edge Transport Barrier (ETB) forms during the transition from low to high confinement (L-H transition) when the heating power reaches a critical value P_c. Such a barrier is characterized by a strong pressure gradient at the plasma edge. The H regime is promising for the next generation of tokamak experiments such as ITER. However, an instability known as Edge Localized Mode (ELM) develops a short time after the threshold P_c is reached. ELMs are characterized by intermittent bursts in the heat flux, therefore causing the transport barrier to relax quasi-periodically. Over the last decade, the possibility of controlling ELMs has become plausible, as recent experiments were carried out on DIII-D, on JET and on TEXTOR [1, 2, 3]. These experimental studies obtained a qualitative control over the ELMs by imposing Resonant Magnetic Perturbations (RMPs) at the plasma edge. However, in order to get any quantitative result, work has to be done in the understanding of ELM dynamics. Recently, elmy-like relaxation oscillations of transport barrier have been obtained using a 3D global electrostatic code of tokamak edge turbulence [4]. We investigate numerically the effects of static RMPs on transport barrier relaxation oscillations. We use the geometry of the TEXTOR tokamak, and plasma parameters close to those used in typical experiments on this machine. In the following, the RBM turbulence model is presented, our numerical results follow, we discuss these results and conclude.

author's e-mail: michael.leconte@univ-provence.fr

2. Resistive Ballooning model

The model used in this study is electrostatic Resistive Ballooning Mode turbulence involving the pressure p and electrostatic potential ϕ. The equations describing this model are the following [4]:

$$\begin{aligned} \frac{\partial \nabla_\perp^2 \phi}{\partial t} + \{\phi, \nabla_\perp^2 \phi\} &= -\hat{G}p - \nabla_\parallel^2 \phi \\ &+ \nu \nabla_\perp^4 \phi \qquad (1) \\ \frac{\partial p}{\partial t} + \{\phi, p\} &= \delta_c \hat{G}\phi + \chi_\parallel \nabla_\parallel^2 p \\ &+ \chi_\perp \nabla_\perp^2 p + S \qquad (2) \end{aligned}$$

The first equation corresponds to the vorticity equation, where $\nabla_\perp^2 \phi$ is the vorticity of the perpendicular (to the magnetic field) component of the $E \times B$ flow, and the parallel current and viscosity effects (ν) are taken into account. The second equation corresponds to energy conservation, where $\chi_\parallel$ and $\chi_\perp$ are collisional heat diffusivities parallel and perpendicular to the magnetic field, and $S = S(x)$ is an energy source modeling a constant heat flux density from the plasma core. Following the standard convention, x represents the local radial coordinate, y is the local poloidal coordinate and z is the local toroidal coordinate, in a magnetic fusion device.

The curvature operator $\hat{G}$ arises from the toroidal geometry of the tokamak, and $\delta_c = \frac{5}{3} \cdot \frac{2L_p}{R_0} \ll 1$ is basically the ratio of the pressure gradient length L_p to the tokamak major radius R_0. In the present model, time is normalized to the interchange time $\tau_{inter} = c_s^{-1} \sqrt{\frac{R_0 \, L_p}{2}}$, which also defines the perpendicular length scale through the ballooning length $\xi_{bal} = \sqrt{\frac{n_{i0} m_i \, \eta_\parallel}{\tau_{inter}}} \frac{L_s}{B_0}$, where c_s is the plasma sound speed, B_0 is the magnetic field strength, n_{i0} is a

reference ion density, m_i is the mass of ions, $\eta_\parallel$ is the parallel resistivity of the plasma and L_s is a reference magnetic shear length.
Note that the parallel gradient is $\nabla_\parallel = \nabla_{\parallel 0} + \{\psi_{RMP}\ ,\ \cdot\}$, where $\nabla_{\parallel 0}$ is the component due to the unperturbed magnetic field, $\{\psi_{RMP}, \cdot\} = \frac{\partial \psi_{RMP}}{\partial x}\frac{\partial}{\partial y} - \frac{\partial \psi_{RMP}}{\partial y}\frac{\partial}{\partial x}$ denotes the Poisson brackets and the magnetic flux due to the resonant magnetic perturbation is written as: $\psi_{RMP}(x,y,z) \sim I_D \sum \psi_m(x) \cos\left(\frac{m}{r_0}y - \frac{n_0}{L_s}z\right)$ where $\psi_m(x) = \frac{\sin[(m-m_0)\Delta\theta_c]}{[(m-m_0)\Delta\theta_c]}\left(\frac{r_0}{r_c}\right)^m \exp\left(\frac{m}{r_0}x\right)$ is the spectrum of the RMPs in slab geometry, m_0 is the central poloidal harmonic number, r_c, $\Delta\theta_c$ denote respectively the radial position and poloidal extension of the RMP-producing coils, n_0 is the toroidal harmonic number and r_0 is a typical radius where the turbulence considered in this paper (resistive ballooning) develops. In the case studied here, we use $r_c = 53.25cm$ and $\Delta\theta_c = 2\pi/5$ for the coils geometry, and we use $n_0 = 4$, with $q_{x=0} = q_0 = 3$, so that the central poloidal harmonic number is $m_0 = 12$. Note that this is a simple matter of choice ($12 : 4$ base mode on TEXTOR-DED [3]), and that the results are valid for any resonant perturbation $\psi_{RMP}(x,y,z)$ of the form given above.

Let the pressure be decomposed into mean part and harmonics: $\bar{p} = \langle p \rangle_{y,z}$, $\tilde{p} = p - \bar{p}$. In a steady-state, equation (2), with conserved total flux $Q_{tot} = \int S(x)dx = \text{Cte}$ and $\delta_c \to 0$, leads to the following equation:

$$\langle Q_{conv} \rangle + \chi_\perp \left| \frac{d\langle \bar{p} \rangle}{dx} \right| + \langle Q_{RMP} \rangle = Q_{tot} \qquad (3)$$

where $Q_{RMP} = \chi_\parallel \langle \frac{\partial \psi_{RMP}}{\partial y} \nabla_\parallel p \rangle_{y,z}$ represents the heat flux due to the magnetic flutter generated by the RMPs, and $Q_{conv} = \langle \tilde{p}\tilde{v}_x \rangle_{y,z}$ is the convective heat flux, where $\tilde{v}_x$ denotes fluctuations of the radial velocity, $\langle \ldots \rangle_{y,z}$ is an average over the poloidal and toroidal directions and $\langle \ldots \rangle$ denotes a time average.

3. Simulation results and discussion

We present time series of the energy content $\int \bar{p}\ dx$ and convective flux Q_{conv}, in presence of an imposed mean sheared flow, for different values of the divertor current I_D [Fig. 1 a-f]. The mean flow $\frac{\partial \phi}{\partial x}$ is artificially forced and the imposed flow profile $V_F(x) = \Omega d \tanh(x/d)$, chosen to be centered at $x = 0$, is strongly sheared with shear rate Ω and shear-layer width d. For comparison, we also performed the same simulations in a case with no mean sheared flow (not shown here), for different values of the divertor current I_D, and also in the following cases: with only self-generated zonal flows, and with suppressed self-generated zonal flows.

In the reference case without RMPs, the energy content increases on a collisional time-scale, until a steady-state is reached, where we observe so-called relaxation oscillations [Fig. 1a], corresponding to a relaxation of the pressure gradient. These relaxations are synchronous to the heat bursts observed on the heat-flux time series [Fig. 1b] and therefore also correspond to relaxations of the transport barrier. We also present time series of the convective flux, in the case without RMPs, for two different values of the shear-layer width d [Fig. 2 a,b]. As seen from the comparison of Fig. 1 and Fig. 2, there is a striking similarity between the effects of a decrease in the shear-layer width d *and* the effects of RMPs on the dynamics of ETB relaxations. Our simulations therefore suggest that the main effect of RMPs in presence of an ETB is to modify the geometrical properties of the ETB, e.g its width, position, etc..., yielding a reduction in the amplitude and frequency of the elmy-like relaxations, and therefore leading to grassy elmy-like relaxations.

In the case with RMPs, the energy content shows that the relaxation oscillations are suppressed by the RMPs , and this suppression is more efficient for higher values of the perturbation current I_D [Fig. 1c,1e]. This suppression of relaxations is also shown as a reduction in the amplitude of the heat bursts and an increase in their frequency.

We also show results for the radial profile of the pressure gradient $|\frac{d\langle \bar{p} \rangle}{dx}|$ [Fig. 3a] and the convective flux Q_{conv} [Fig. 3b], in presence of an imposed mean sheared flow, for different values of the divertor current I_D.

In the reference case without RMPs ($I_D = 0$) but with a mean shear flow ($\Omega = 4$), the convective flux Q_{conv} [Fig. 3b] is reduced around the position $x = 0$ compared with a case with no mean sheared flow. A high pressure gradient $|\frac{d\langle \bar{p} \rangle}{dx}|$ around this position, also referred to as an Edge Transport Barrier (ETB) is created at the position of maximal flow-shear $x = 0$ [Fig. 3a]. The appearance of this strong pressure gradient is linked to a severe reduction in the convective heat flux Q_{conv} by the mean sheared flow as seen from the conservation of energy (3) with $Q_{RMP} = 0$:

$$\langle Q^0_{conv} \rangle + \chi_\perp \left| \frac{d\langle \bar{p}^0 \rangle}{dx} \right| = Q_{tot} \qquad (4)$$

where the superscript 0 indicates the reference case without RMPs ($I_D = 0$).

In the case when there is a combination of a mean shear flow ($\Omega = 4$) *and* RMPs ($I_D \neq 0$), the ETB due to the mean shear flow (and enhanced by the RMPs) is eroded in the vicinity of the position $x \sim 0$, compared

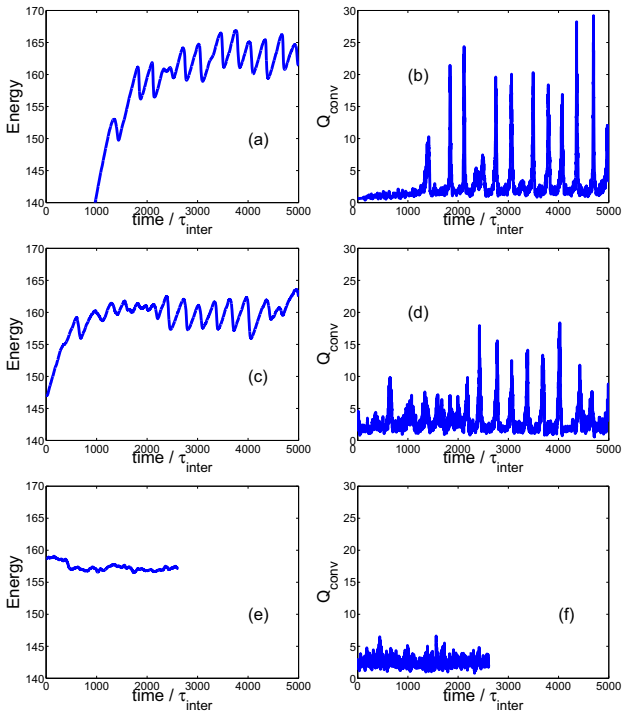

Fig. 1 Effects of RMPs on the dynamics of barrier relaxations: time traces of the thermal energy (a,c,e) and the radial heat flux (b,d,f), in presence of an imposed mean shear flow with shear rate $\Omega = 4$, for (a, b) no RMP perturbation, (c, d) $I_D = 0.5\ kA$ and (e, f) $I_D = 1\ kA$.

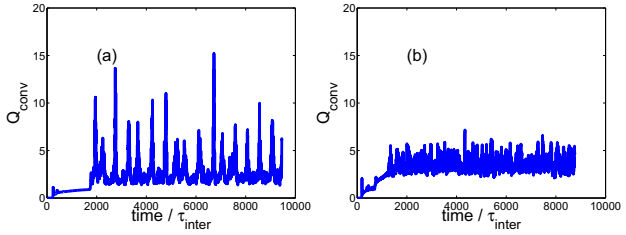

Fig. 2 Effects of width d of the shear-layer on the dynamics of barrier relaxations: time traces of the radial turbulent flux, in the case without RMPs, in presence of an imposed mean sheared flow with shear rate $\Omega = 2$, for $a)$ $d = 20\%$ and $b)$ $d = 10\%$.

to the case without RMPs [Fig. 3a]. This erosion of the ETB only appears when both a mean shear flow and RMPs are present, and therefore can be explained by a synergetic effect.

We propose the following model based on the balance of heat fluxes, to explain the behaviour of the convective flux and pressure gradient in the presence of RMPs and a shearflow-induced transport barrier. Taken into account RMPs, the pressure harmonics can be further decomposed into an equilibrium and a turbulent part: $\tilde{p} = \tilde{p}^{eq}(x, y, z) + \tilde{p}^{turb}(x, y, z, t)$, and similarly for the radial velocity harmonics $\tilde{v}_x$. The energy

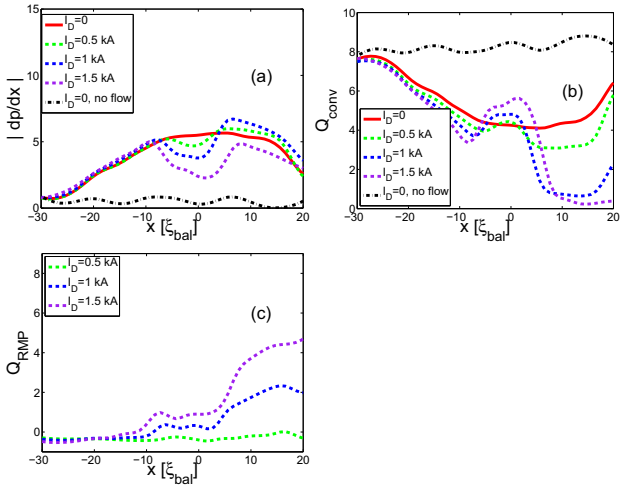

Fig. 3 Effects of resonant magnetic perturbations on: (a) the pressure gradient and (b,c) radial heat fluxes, for different values of the perturbation current I_D. Q_{conv} denotes the convective heat flux and Q_{RMP} is the conductive heat flux induced by the resonant magnetic perturbations. The total heat flux is $Q_{tot} = 10$.

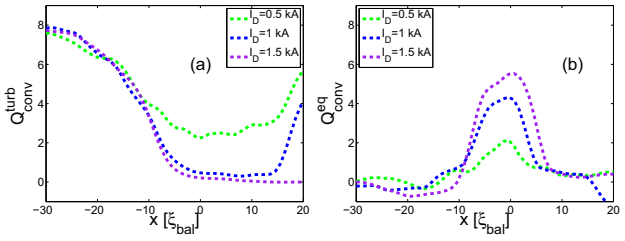

Fig. 4 Components of the radial convective flux: (a) turbulent convective flux Q^{turb}_{conv}, and (b) equilibrium convective flux Q^{eq}_{conv}, e.g. RMP-linked, for different values of the perturbation current I_D. The total heat flux is $Q_{tot} = 10$.

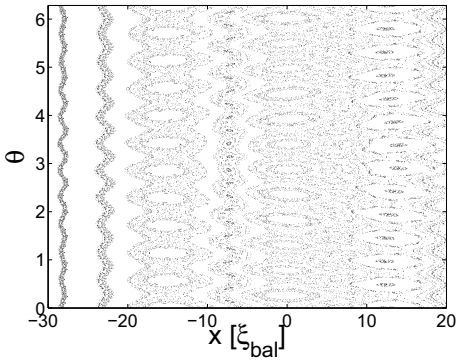

Fig. 5 Effects of RMPs on the topology of magnetic field lines: Poincare map for a perturbation current of $I_D = 0.5\ kA$. There is clear evidence of residual magnetic island chains, and stochasticity in between them.

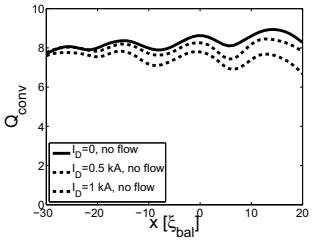

Fig. 6 Effects of RMPs on the convective heat flux, in the case where the mean flow is artificially suppressed.

balance (3) can then be written:

$$Q^{eq}_{conv}+\langle Q^{turb}_{conv}\rangle+\chi_\perp\left|\frac{d\langle\bar{p}\rangle}{dx}\right|+\langle Q_{RMP}\rangle = Q_{tot} \quad (5)$$

where $Q^{eq}_{conv}(x) = \langle\tilde{p}^{eq}\tilde{v}^{eq}_x\rangle_{y,z}$ is the equilibrium convective flux and $Q^{turb}_{conv}(x,t) = \langle\tilde{p}^{turb}\tilde{v}^{turb}_x\rangle_{y,z}$ is the turbulent convective flux. Radial profiles of the equilibrium convective flux and of the (time-averaged) turbulent convective flux are shown for different values of the perturbation current I_D [Fig. 4].

Because of the presence of localized residual island chains (as seen on Figure 5), depending on the region considered, there are three different limits:

i) Close to the resonant surface $x = 0$, e.g. $|x| \ll \frac{w}{2} \ll d$, where $w \sim 2\sqrt{I_D}$ is the magnetic island chain width and d is the shear-layer width of the mean flow (chosen to be centered at $x = 0$), the turbulent convective flux is reduced by the sheared flow and additionnally reduced by RMPs due to stochastic transport [Fig. 5 and 6] so that $\langle Q^{turb}_{conv}\rangle/Q_{tot} \ll 1$ [Fig 4a], and an equilibrium convective flux Q^{eq}_{conv} indirectly linked to RMPs appears [Fig. 4b]. This equilibrium convective flux is a consequence of the presence of an RMP-induced residual magnetic island chain at the radius $r = r_0 = 0.45\ [m]$ corresponding to the position $x = 0$ [Fig 5]. Moreover, the RMP induced flux is low in the vicinity of $x = 0$: $\langle Q_{RMP}\rangle/Q_{tot} \ll 1$ [Fig. 3c]. Therefore, the energy balance (5) simplifies to: $Q^{eq}_{conv} + \chi_\perp\left|\frac{d\langle\bar{p}\rangle}{dx}\right| \sim Q_{tot}$ so that, in the region $x \sim 0$, the appearance of the equilibrium convective flux Q^{eq}_{conv} must be balanced by a decrease in the pressure gradient, seen on Figure 3a, similar to a flattening of the pressure profile that occurs in the study of plasma macroinstabilities [5].

ii) For x negative, far from the resonant surface, e.g. $x \ll -\frac{w}{2} \ll -d$, the RMP-linked equilibrium convective flux is small $Q^{eq}_{conv}/Q_{tot} \ll 1$, since there is no residual island chain in this region, so it does not play any role. The turbulent convective flux $\langle Q^{turb}_{conv}\rangle$ is reduced by the mean-shear flow. Moreover, the RMP-induced flux Q_{RMP} is small in this region $\langle Q_{RMP}\rangle/Q_{tot} \ll 1$. Therefore, the energy balance (5) reduces to:

$$\langle Q^{turb}_{conv}\rangle + \chi_\perp\left|\frac{d\langle\bar{p}\rangle}{dx}\right| \sim Q_{tot} \quad (6)$$

Moreover, in this region, the turbulent convective flux does not depend on the perturbation current I_D [Fig. 4a], because the magnetic field lines are not stochastic [Fig. 5], so for $x \ll -\frac{w}{2} \ll -d$, we have $\langle Q^{turb}_{conv}\rangle \sim \langle Q^{0}_{conv}\rangle$ and therefore equations (4) and (6) imply: $\left|\frac{d\langle\bar{p}\rangle}{dx}\right| \sim \left|\frac{d\langle\bar{p}\rangle^0}{dx}\right|$. Thus the pressure gradient profile is only weakly modified by the RMPs in the region $x \ll -\frac{w}{2} \ll -d$ [Fig. 3a].

iii) For x positive, far from the resonant surface, e.g. $\frac{w}{2} \ll x \ll d$, the equilibrium convective flux is small ($\langle Q^{eq}_{conv}\rangle$), since there is no residual island chains. The energy balance (3) thus reduces to: $\langle Q^{turb}_{conv}\rangle + \chi_\perp\left|\frac{d\langle\bar{p}\rangle}{dx}\right| + \langle Q_{RMP}\rangle \sim Q_{tot}$. An increase in the perturbation current I_D causes an increase in the RMP-induced heat flux $\langle Q_{RMP}\rangle$, but it induces also a decrease in the turbulent convective heat flux $\langle Q^{turb}_{conv}\rangle$, linked to stochastic transport [Fig. 4a].

In this region, there is therefore a competition between the $\langle Q_{RMP}\rangle$ and $\langle Q^{turb}_{conv}\rangle$ heat fluxes, which may explain the fact that, in the region $\frac{w}{2} \ll x \ll d$, the pressure gradient increases for small perturbation currents and decreases for higher perturbation currents [Fig 3a].

4. Conclusions

In this work, we investigated the effects of Resonant Magnetic Perturbations (RMPs) on transport barrier relaxations. It is shown that RMPs have a stabilizing effect on these relaxations, and that this effect is linked to a modification of the pressure gradient equilibrium profile due mainly to the formation of magnetic island chains. An erosion of the pressure gradient profile is observed at the surface of principal resonance, e.g at the rational surface $q = m_0/n_0$, where $m_0,\ n_0$ are the principal poloidal wave-number

and the toroidal wave-number of the RMPs, respectively. This erosion is shown to be linked to the presence of residual magnetic island chains inducing a stationnary convective transport of heat (and particles) in the radial direction. Far from the principal resonance surface but inside the shear-layer, the pressure gradient modifications are only linked to the presence (or not) of stochastic resonance overlap.

[1] T.E. Evans, R.A. Moyer, P.R. Thomas et al., *Phys. Rev. Lett.* **92**, 235003 (2004).
[2] Y. Liang, H.R. Koslowski, P.R. Thomas et al., *Phys. Rev. Lett.* **98**, 265004 (2007).
[3] K. H. Finken, B. Unterberg, Y. Xu et al., *Nucl. Fusion* **47**, 522 (2007).
[4] P. Beyer, S. Benkadda, X. Garbet et al., *Plasma Phys. Controlled Fusion* **44**, 2167 (2002).
[5] R. Fitzpatrick, *Phys. Plasmas* **2**, 825-837 (1995).